Biomass and Bioenergy 122 (2019) 414–425

Contents lists available at ScienceDirect

Biomass and Bioenergy

journal homepage: www.elsevier.com/locate/biombioe

Review

Estimation methods developing with remote sensing information for energy crop biomass: A comparative review

Zhenhua Chao[a], Ning Liu[b], Peidong Zhang[b,*], Tianyu Ying[c], Kaihui Song[d]

[a] School of Geographic Science, Nantong University, Nantong, 226007, China
[b] College of Environment and Safety Engineering, Qingdao University of Science & Technology, Qingdao, 226042, China
[c] School for Environmental and Sustainability, University of Michigan, Ann Arbor, 48109, MI, USA
[d] Department of Geographical Science, University of Maryland, College Park, 20742, MD, USA

ARTICLE INFO

Keywords:
Energy crop biomass
Vegetation index
SAR
NPP
Crop height
Data assimilation

ABSTRACT

The rapid development of remote sensing (RS) technology enables an increased usage of high - resolution, spatial, temporal or spectral, data to extract vegetation information, improve model parameters, and estimate energy crop biomass accurately. Five estimation methods developing with RS information for energy crop biomass are summarized in this paper. Firstly, the statistical analysis with vegetation index can be regarded as the commonest method. But it is faulted for the deficiency of sample data and the vulnerability to the influence of many factors such as cloudy days. Secondly, the longer wavelength makes SAR information popular for crop biomass estimation. But many limitations lead to measurement uncertainty and bring about poor classification. Thirdly, NPP can directly reflect accumulated biomass production through photosynthesis and measure the consequences caused by climate change and human activities. But, actual LUE, the results of environmental stresses such as light intensity, temperature, water, and nutrients, is usually considered as a constant. Fourthly, crop height information is vitally important for biomass estimation. Yet the corresponding application is often subject to many factors e.g. crop variety, growth period, and farmland management practices limits. Lastly, the most promising approach lies in the possibility of assimilating state variables from RS data into CGMs. And the advent of latest instruments with better characteristics offer a unique chance to overcome current limitations. In the end, the main challenges and opportunities for energy crop biomass estimation using RS information in the future are listed.

1. Introduction

Biomass from energy crops is a very versatile resource that can be used to produce heat, electricity, and transport fuels etc. and the future demand is projected to achieve substantial growth. Energy crops including both food and energy crops could potentially supply about 435 EJ yr^{-1}, exceeding the whole primary energy supply over the world [1]. But the potential contribution of biomass to future energy supply globally exists widely due to two key variables, land availability and yields of energy crops [2]. Despite the doubts on its potential and the heated debate on passive social and ecological effects on food security, farmers' livelihood and biodiversity preservation due to the large-scale conversion of land from production of food and feed into energy crops, a common point of view is that production of energy crops is the main way to alleviate greenhouse gas emissions as it can replace the need for fossil fuel usage [3,4].

Studies show that the yield characteristics of energy crops are different at different growth stages [5,6]. In addition, it takes efficient management strategies to convert agricultural food, fiber and energy crop cultivation worldwide into an ecological, economical and sustainable production process. Several factors should be identified and addressed, including land resources, spatial distribution of resources, geographic factors of the resources, and an absorptive capacity of a proximal infrastructure, to assess the spatial distribution and quantity of energy crop biomass accurately. Continuous temporal and spatial information on crop status is an essential prerequisite for the successful applications of these strategies [7,8]. Geo-technology i.e. remote sensing (RS), geographic information system (GIS), and global positioning system (GPS) and data mining techniques can identify the spatial information effectively and so producers will ensure maximum crop yield under favorable conditions [9–13]. The primary reason for using RS data, apart from the ability to cover large areas, is its ability to offer useful information on crop activity and health in a practical non-destructive way [14–16].

* Corresponding author.
E-mail address: wood0349@163.com (P. Zhang).

https://doi.org/10.1016/j.biombioe.2019.02.002
Received 17 August 2018; Received in revised form 2 February 2019; Accepted 4 February 2019
Available online 14 February 2019
0961-9534/ © 2019 Published by Elsevier Ltd.

Abbreviations

AGB	aboveground biomass
ALOS	Advanced Land Observation Satellite
ANPP	aboveground net primary productivity
APAR	absorbed photosynthetically active radiation
ASAR	advanced synthetic aperture radar
ATLS	autonomously operating terrestrial laser scanning
AVHRR	Advanced Very High-Resolution Radiometer
CASA	Carnegie-Ames-Stanford-Approach
CASI	Compact Airborne Spectrographic Imager
CCD	charge-coupled device
CGMs	crop growth models
CSM	crop surface model
DA	data assimilation
DSSAT	Decision Support System for Agro-technology Transfer
EnKF	Ensemble Kalman filter
EVI	enhanced vegetation index
fPAR	the fraction of photosynthetically active radiation
GAI	green area index
GIS	geographic information system
GLO-PEM2	Global Production Efficiency Model Version 2.0
GPP	gross primary productivity
GPS	global positioning system
JERS-1	Japanese Earth Resources Satellite-1
LAI	leaf area index
LiDAR	light detection and ranging
LUCC	land use and land cover change
LUE	light use efficiency
MODIS	Moderate Resolution Imaging Spectrometer
NDVI	normalized difference vegetation index
NIR	near-infrared
NPP	net primary productivity
PLS	partial least square regression
Pol-InSAR	Polarimetric SAR Interferometry
RGB	red green blue
RS	remote sensing
SAFY	simple algorithm for yield estimate
SAR	synthetic aperture radar
SAVI	soil-adjusted vegetation index
SFCR	Sub-foliage corner reflector
SIF	solar-induced chlorophyll fluorescence
SIR-C/X-SAR	Spaceborne Imaging Radar-C/X-Band Synthetic Aperture Radar
STICS	Simulateurmul TI discplinaire pour les Cultures Standard
TLS	terrestrial laser scanners
UAS	unmanned aerial systems
UAV	unmanned aerial vehicle
VI	vegetation index
WOFOST	WorldFOodSTudies

Nomenclature

EJ	exajoule, equal to one quintillion joules
Km	kilometer
nm	nanometer

2. Objective

The rapid development of RS has led to increasing usage of high-resolution data regarding space, time and spectrum to extract vegetation information and improve parameters, which enables the timely energy crop biomass estimation with increased accuracy. With the increasing applications of spaceborne RS in grassland management, Ali et al. [17] reviewed the relevant methods and applications based on satellite remote sensing data and identified the current main challenges and new forthcoming trends in the future. The instruments of RS have a wide range, from airborne cameras to sensors onboard satellite. A better understanding of the relationship between leaf reflectance changes and physio-ecological factors of vegetation has been achieved with the development of RS methods. Available remote sensing platforms, satellite, aerial and ground, offer different spatial- and temporal-resolution information for energy crops management. The ground-based RS data excels in establishing the calibration model for biomass yield prediction and providing references for aerial and satellite RS which are good at covering a wide range of biomass production systems [18].

The applications of RS have received considerable attention in estimating crop biomass since the advent of RS (Fig. 1). Along with increasing RS information from various RS systems, the amount of biomass estimation methods for energy crops keeps growing. And the existing methods have their strengths and weaknesses. However, few papers offer a systematic review of widely used estimation methods with RS information. Here, this paper summarized existing different energy crop biomass estimation methods with RS information and then compared the pros and cons of these typical methods. The main challenges and forthcoming trends for future development are also outlined.

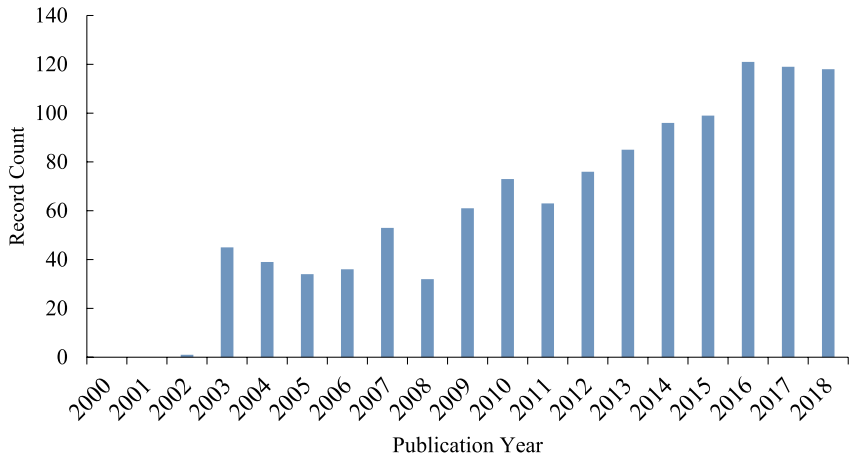

Fig. 1. Statistics about publication on topic 'remote sensing' AND topic 'biomass' AND topic 'crop' searched via Web of Science since 2000.

3. Estimation methods with RS information

Each estimation method for biomass with RS information is developed on a certain mechanism. Generally, the existing methods can be divided into five categories, which are, 1) the simple statistical analysis with vegetation indices, 2) the method based on SAR data, 3) the net primary productivity estimation method with RS information, 4) the crop height -based estimation method, and 5) the crop growth model method with RS information.

3.1. Simple statistical method with vegetation indices

3.1.1. Introduction of vegetation index

Electromagnetic radiation in the visible spectrum (wavelength = 400–700 nm) is absorbed by plant pigments in typical green vegetation. Relatively less absorption occurs in the green band (500–600 nm), which creates a "reflectance peak" in this region resulting in the green coloration of plants as perceived by the human eye. The spongy mesophyll cells are associated with pronounced scattering of near-infrared (NIR) radiation, causing a typical high spectral reflectance in the 700–1200 nm region of the spectrum (Fig. 2). The spectral reflectance in the red region for healthy, actively growing vegetation typically diminishes as plants grow (because of increasing photosynthetic activity, absorption at that wavelength is greater), while the NIR reflectance increases steadily with increasing amounts of the canopy. Increases in leaf thickness may also be correlated with increases in NIR reflectance. Because of the reflectance responses of vegetation within the red and NIR portions of the spectrum (as related to the chlorophyll content and canopy architecture of a plant, respectively), data acquired from these two regions have been widely used to create spectral transformations which are generally referred to as "vegetation indices" (VIs) or broadband VIs. These numerical indices provide partially analytical gauges on vegetation activity, capable of revealing the seasonal variations of the green plant for different space scales. These indices are often used to detect the spatial variability of crops, especially of precision agriculture [19–30] and derive crop biophysical characteristics e.g. LAI (leaf area index) routinely [20,31–34].

Red edge located within 680–750 nm is affected by leaf chlorophyll content, that is, the rise of reflectance at the edge lying in the range between the red wavelengths and the NIR wavelengths indicates the red edge (Fig. 2) [19,35–37], usually regarded as narrowband VI. As plants grow vigorously, the spectral reflectance of the canopy in certain spectrum range will be asymptotic, making broadband VIs less effective. By contrast, the novel narrow band indices can reduce the phenomenon and have a distinct advantage in estimating biomass at high-density vegetation [35,38,39]. Nowadays, the red edge channel can be obtained operationally with RapidEye, the first higher solution multispectral RS system. Furthermore, hyperspectral RS enables VIs to be investigated on the basis of narrow bands in 350–2500 nm instead of focusing on broad bands such as the red and NIR alone, offering distinctive narrow bands to define new VIs for a particular species and/or parameter and providing suitable spectral resolution and sufficient information concerning the biochemical composition and biophysical structure of vegetation canopies [40–42].

Spectral responses of different crops at various growth stages often differ greatly and corresponding spectral models can be built for biomass resources management [43,44]. So far a large number of indices including broadband VI and narrowband VI have been developed, as shown in Table 1.

3.1.2. The application of simple statistical estimation method with VIs

A large number of biomass estimations with VI information have been carried out. Results of multiple studies show that strong correlations between biomass measured and satellite-derived VIs exist [57,58]. Based on such a relationship, the simple statistical analysis can be established to estimate energy crop biomass with the most suitable VI and optimal regression results. To make the missing biomass data perfect in counties where National Agricultural Statistics Service-reported yields are unavailable, Lokupitiya et al. [59] used CCA (canonical correlation analysis) and best subset multiple regressions to estimate AGB with Pathfinder biweekly NDVI in Iowa. Claverie et al. [60] coupled the SAFY (simple algorithm for yield estimate) model with the Formosat-2 data for crop production estimation over large areas. The SAFY model performed better for biomass estimation by using the crop phenology-related parameters which were derived through spatio-temporal fusion of Landsat-8 images and MODIS images [61]. Wang et al. [62] evaluated the use of HJ-1 CCD-derived VIs for monitoring ongoing rice growth over the years and explored the common statistical models and nonparametric methods for retrieving LAI and AGB on the basis of a wide range of field measurements. The relationships between the VIs

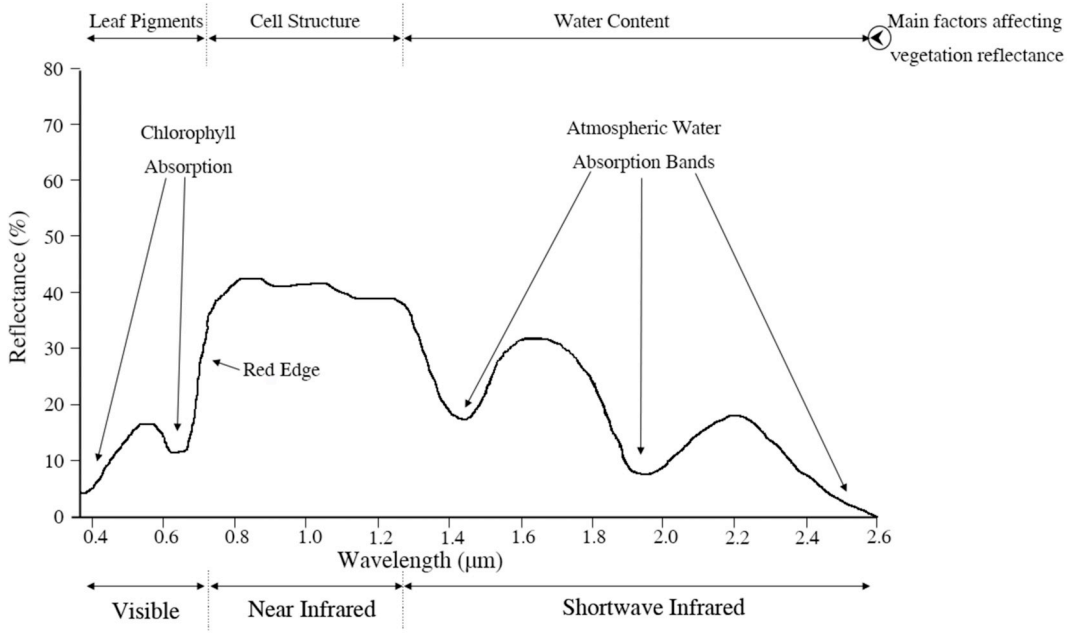

Fig. 2. The spectral reflection curve of green plants.

Table 1
Equations used to calculate VIs.

Vegetation Index	Formulation	Reference
Simple Ratio	$SR = \rho_{NIR}/\rho_{Red}$	[45]
Normalized Difference Vegetation Index	$NDVI = (\rho_{NIR} - \rho_{Red})/(\rho_{NIR} + \rho_{Red})$	[46]
Enhanced Vegetation Index	$EVI = 2.5\frac{\rho NIR - \rho Red}{1 + \rho_{NIR} + 6\rho_{Red} - 7.5\rho_{Blue}}$	[47]
Green Atmospheric Resistant Vegetation Index	$GARI = \frac{\rho NIR - (\rho_{Green} - \gamma(\rho_{Blue} - \rho Red))}{\rho_{NIR} + (\rho_{Green} - \gamma(\rho_{Blue} - \rho Red))]}$	[48]
Wide-Dynamic Range Vegetation Index	$WDRVI = \frac{\alpha \cdot \rho NIR - \rho Red}{\alpha \cdot \rho NIR + \rho Red}$	[49]
Green Chlorophyll Index	$CI_{\text{Green}} = \frac{\rho NIR}{\rho Green} - 1$	[50–52]
Red-edge Chlorophyll Index	$CI_{\text{Red}-\text{edge}} = \frac{\rho NIR}{\rho Red-edge} - 1$	[50–52]
MERIS Terrestrial Chlorophyll Index	$MTCI = \frac{\rho NIR - \rho Red-edge}{\rho Red\ edge - \rho Red}$	[53]
Soil-Adjusted Vegetation Index (SAVI)	$SAVI = \frac{\rho NIR - \rho Red}{\rho_{NIR} + \rho_{Red} + L}(1 + L)$	[54]
Modified Soil Adjusted Vegetation Index (MSAVI)	$MSAVI = \frac{2\rho NIR + 1 - [(2\rho NIR + 1)^2 - 8(\rho NIR - \rho Red)]^{0.5}}{2}$	[55]
Difference Vegetation Index	$DVI = \rho_{NIR} - \rho_{Red}$	[56]

Where ρ_{NIR} = crop reflectance in the near infrared band, ρ_{Red} = crop reflectance in the red band, ρ_{Blue} = crop reflectance in the blue band. L is the soil-adjustment factor.

and rice growth parameters are robust and the cumulative VIs perform well at estimating total dry AGB. As Stagakis et al. [63] argued, the reflectance in the visible and NIR spectrum for the canopy is inseparably intertwined with both canopy biophysical properties such as the number of leaves per area and canopy biochemical features e.g. chlorophylls and carotenoids. It is impossible to develop an exclusive VI especially sensitive to a plant variable. Moreover, most VIs are only suitable for several special species and consequently have no distinct effect when applied to different species with diverse canopy architectures and leaf structures [64]. NDVI (normalized difference vegetation index), a most popular index, has an acute sensitivity to low LAI. The productivity in the growing season can be estimated accurately and the variation in evergreen biomass could be easily detected with NDVI [65]. But this indicator tends to saturate at medium to high degree of LAI (e.g. Ref. [32]). A similar pattern between NDVI and biomass is also obvious, with the index saturating at medium to high biomass (about 2 kg/m^2, e.g. Ref. [66]). Furthermore, background soil reflection, atmospheric and water absorption etc. usually have negative effects on the estimation accuracy of crop biomass, which is very common with broadband VIs.

When considering hyperspectral RS for estimating total wheat biomass and LAI, the relationship between the red edge and wheat biomass is particularly notable [67]. A specific narrow band with the longer wavelength in red can be used as a significant signal to characterize agricultural crop biophysical properties with several crops' ground-level hyperspectral reflectance measurements e.g. cotton, potato, soybeans, corn, and sunflower [68]. It must be said that the red edge indices have no significant improvement in estimating LAI and biomass of corn and soybean with different vegetation characteristics over traditional multispectral indices. While a combination of RapidEye, Landsat and SPOT data and sensor-dependant best-fit functions could improve continuous crop LAI monitoring over time and space at the field level [69,70]. The ratio VI computed by the sum of 1st derivative value within red edge and the blue edge as input variables made the estimation model as the best one for fresh rice biomass [71]. With hyperspectral data, the random forest models are proved to be most useful in retrieving LAI and AGB for coastal marshes in Louisiana [72]. Band depth analysis parameters outperform the application of traditional VIs such as NDVI, SAVI for grassland biomass and nitrogen density [73]. However, hyperspectral data has no advantage over multispectral data for vegetation cover and AGB modeling when testing if hyperspectral data outperforms multispectral data in estimating vegetation cover and AGB on the Qinghai-Tibet Plateau [74].

3.1.3. Limitations of the simple statistical method with VIs

It is an effective way to estimate biomass with a VI characterized by simplicity, availability, interpretability, and acceptance. But a simple statistical estimation method with a VI requires a large number of sample data. And it is very difficult to find a satisfactory compromise between the simplified models and higher accuracy due to the use of poor information [75]. Besides, the vegetation spectrum is often affected by vegetation growth state, environmental conditions and other factors. So the method is non-universal for different crops across different regions. Energy crop biomass estimation method based on hyperspectral bands can take full advantages of the spectral dimension and consider canopy reflectance of different responses during the growth of crops. But what limits a VI's application to different crops at other regions is that different growth process cannot be expressed by one VI. One of the primary challenges to assess vegetation parameters is how to minimize the impacts of external factors and make the relationship between VIs and biophysical parameters most sensitive. The main disadvantage is that the data from chaotic systems in the nonlinear dynamic environment cannot meet the primary assumptions of a linear model. Significantly, cloud cover limits the use of VI information too [76–79]. Furthermore, the estimation accuracy is not high enough to meet the actual output as the asymptotic saturation is common for passive optical sensors [80,81].

Consequently, the relationships between spectral information and biomass are restrained because it is very hard to apply the spatial and temporal transferability of RS data and the corresponding recalibration is often frequent and costly. The reliable spatial scale and spatial pattern could improve the estimation accuracy of aboveground biomass (AGB) [82,83], while the concern in the quantitative analysis is how to measure surface characteristics using RS data with different spatial resolutions [84].

3.2. The estimation method based on SAR data

Normally, cloudy days limit the application of data from optical sensors in estimating energy crop biomass. By contrast, microwave emission collected by passive sensors and backscatter from radars, suitable for almost all-weather conditions, are sensitive to the water content of biomass and radar data can be directly used to estimate AGB.

3.2.1. Types and application of SAR data

As a form of radar, synthetic aperture radar (SAR) can be used to measure the distance and transmitted/backscattered radiation of the

target scene. Given its all-weather capability, SAR response is largely dependent upon crop structure and given differences in structure among crop canopies, fields. A number of SAR instruments are being used for vegetation phenology. For instance, TerraSAR-X and the COSMO–SkyMed constellation were used by Hajj et al. [85] to carry out the sensitivity study of radar signals to soil moisture and vegetation parameters within irrigated grassland fields. The Japanese ALOS and ALOS-2 L-band instruments, and ESA ASAR (Advanced Synthetic Aperture Radar) and Sentinel-1 C-band platforms, having a lower spatial resolution but with a longer wavelength, were more susceptible to vegetation volume in distinguishing among grassland types in Ireland [86]. Different wavelengths have different sensitivity to vegetation conditions [87,88]. Metz et al. [89] demonstrated that the combined usage of a TerraSAR-X and Radarsat-2 time series was most accurate at discriminating Europe Natura 2000 protected site from high nature value habitats. With variety wavelengths, it is feasible to exploit different polarimetric acquisition capabilities. For example, a TerraSAR-X dual polarimetric SAR time series was used to detect grassland cutting practices [90], and a combination of multi-angle Radarsat-2 quad-polarization images improved grassland classification results compared with the individual incidence angles [91]. The relationship between L-band SAR backscatter and dense tropical forest biomass showed that SAR backscatter correlates negatively with forest biomass once reaching a maximum value [92]. A new approach to estimate LAI by the coupling of the Water Cloud Model and Ulaby model was developed with multi-polarization RADARSAT-2 (C-band) and UAV SAR (L-band) for major crops, corn and soybeans, in Canada. It turned out that SAR with an all-weather acquisition capability can estimate LAI and monitor crop growth operationally [93].

3.2.2. Energy crop biomass estimation method based on SAR data

Experimental research has demonstrated that the microwave backscattering coefficient, affected by the shape and dimensions of plant constituents, is sensitive to crop biomass. The L-band seems to be the most convenient frequency band for studying the contribution from “broad leaf” crops, while a higher frequency (C-band) is suitable for “narrow leaf” crops. The relation between vegetation characteristics and model state variables describing the microwave attenuation shows that the Pol-InSAR (Polarimetric SAR Interferometry) parameters are sensitive to canopy structure and biomass. However, this sensitivity is dependent on crop types and radar frequency [94].

Considering that most rice grow in rainy season, rice paddy fields monitoring is of particular significance with the all-weather capability of SAR since the synergistic use of SAR sensors with diverse frequency is sensitive to different canopy characteristics [95,96]. It was found that the correlation between the panicle biomass, one of the various canopy properties, and backscattering coefficient values from two current X-band SAR sensors, COSMO-SkyMed and TerraSAR-X, is the highest. It is promising to assess rice grain yields directly by using X-band SAR at regional scales, whereas the limitation is that such SAR is not good at assessing the whole-canopy properties at the very early growth stages [97]. A nonlinear trend between dry biomass and radar responses is apparent in many cases. The tendency of SAR response rises more rapidly earlier in the season when biomass accumulation speeds up. During the mid to late season, a reduced rate of increase in SAR response is obvious when crops are at the stage of seed and fruit [98]. Normally, plant geometry could explain that crops with different backscattering coefficients have same biomass [99–101]. Bivariate correlation results indicated that both multi-temporal EO-1 Hyperion and Envisat ASAR data could justify remarkable relations with crop conditions for winter wheat fields. A multiple regression analysis as a function of crop parameters based on the combination of hyperspectral indices and microwave backscatter improves the crop parameter estimation. The performance for biomass estimation is better than any single one in prediction power [102].

3.2.3. Advantages and disadvantages of the estimation method with SAR data

One special property of SAR is that the longer wavelength can penetrate through cloud cover, haze, dust, and all but the heaviest rainfall, making microwave under almost all weather and environmental conditions detectable. In practice, data from the existing spaceborne SAR systems such as ASAR, RADARSAT-2, ALOS-1 and NASA/JPL AIRSAR are popular for crop biomass estimation at regional scales.

Microwave penetration depends on the wavelength and incident angle. L-band with longer wavelengths penetrate further into crop canopy than C-band. L-band wavelengths responses arise from greater canopy-soil interaction and the scattering directly from the soil whereas the correlation between C-band microwaves and the upper canopy is stronger [93,103,104]. When considering the discrepancies between Pol-InSAR and SFCR (Sub-foliage corner reflector) loss estimation, a hypothetical possibility is that temporal changes in the reference radar cross section may overestimate the loss factors from SFCRs, without any support of quantitative evidence support [94]. Still, the work done in the microwave domain is constrained by a lot of limitations, especially in distinguishing the signal response of vegetation cover or moisture and acquisition conditions. The inherent speckle noise of SAR data leads to a loss of some details that may increase measurement uncertainty and bring about poor classification. In order to overcome various restrictions and strive to verify the results, intensive ground-based measurements or speckle reduction filters such as a spatial filter, temporal filters are typically required [105–108].

In mountainous regions, a major limitation is that the topography has negative effects on geometry and radiation e.g. radar shadow by foreshortening and layover when mapped to ground-range images [109]. Moreover, the rain or heavy clouds can disturb the microwave signal-propagation and/or the physical changes in land surfaces and so the quality of SAR data, especially in high-frequency bands such as Ka, Ku, and X can be affected under such weather conditions [110]. Furthermore, it is still challenging to obtain SAR data with appropriate time series or even a single observation in many parts of the world for relatively high energy on satellite platforms needs to be provided to support SAR work. Satellite-based SAR data characterized by the low spatial and temporal resolution limit the use for large-scale multi-temporal assessments [111]. To some extent, the recently launched satellite missions, C-band Sentinel-1 and L-band ALOS-2, may improve this condition [112]. Last but not least, the insensitivity or saturation of remotely sensed signals at moderate to high biomass levels is still one of the main challenges for radar data [113].

3.3. Net primary productivity estimation method

CO_2 from the atmosphere absorbed by plants through photosynthesis is usually representative of vegetation productivity. During the process, sunlight is converted into chemical energy by green plants and the organic dry matter is produced. Vegetation primary productivity is commonly divided into two types: gross primary productivity (GPP) and net primary productivity (NPP). GPP is the overall rate of biomass production in ecosystem scale, whereas NPP is the biomass produced after accounting for energy lost to cellular respiration and maintenance of the plants, directly reflecting the production capacity of plant communities [114–116]. That is, the gross biomass for energy crop can be expressed as cumulative NPP during the growing period.

3.3.1. The classification of NPP estimation method

Models used to calculate NPP are generally grouped into the climate-related model, light use efficiency (LUE) model and process-based model. The way to estimate biomass accumulation cannot be reflected by climate-related model, namely, statistical method spatially explicit when analyzing the effects of natural factors and/or human activity on biomass accumulation [117–119]. By comparison, process-based terrestrial ecosystem models do express the impact of corresponding

factors on biomass accumulation more explicit. Based on the different physical understandings of the process, the process-based model takes soil, temperature, and climatic variables into account for NPP estimation. However, current studies indicate that the performances of the process-based model are poor due to the significant differences between observed values and model estimations [120,121]. Among all these models, characterized by the simplicity of concepts, the potential is great to use LUE models to estimate the spatiotemporal dynamics of NPP accurately with a rich supply of RS data [122].

3.3.2. LUE model

Various LUE models such as Carnegie-Ames-Stanford-Approach (CASA) and the C-Fix model have been developed. LUE can take the constraints imposed by environmental factors, for example, light intensity, temperature, and nutrients into account. In an LUE model, NPP can be quantified as a function of APAR (absorbed photosynthetically active radiation) by light use efficiency ε as formula (1). The ε, a plant- or biome-specific value, gives consideration to the concentration of CO_2, temperature, solar radiation, and fPAR (the fraction of photosynthetically active radiation absorbed by vegetation).

$$NPP = APAR\Delta \cdot \varepsilon \quad (1)$$

Apart from leaf structure, day length and potential incident radiation vary greatly in different regions as well as weather conditions, so APAR changes accordingly. APAR can be extracted from photosynthetically active radiation (PAR). The amount of solar radiation reaching the canopy, PAR, is usually derived from RS data or computed with common mathematical algorithms [123,124]. With RS data, some vegetation properties can be derived over the entire area and NPP can be estimated for each pixel in the study area, so formula (1) can be expressed as formula (2).

$$NPP = (fPAR \cdot PAR) \cdot \varepsilon \quad (2)$$

Both models, the CASA and Global Production Efficiency Model Version 2.0 (GLO-PEM2), inclined to underestimate maize yields all over China and the difference between the models was not obvious in both estimated production and spatial patterns. Comparatively, the CASA model did better in the areas with dense crop [125]. And NPP estimated by the CASA model tended to have a high correlation with rice yield [126]. A decision-support model was used successfully to measure the usable biomass for generating bio-fuel based on the amounts and spatial distribution of biomass residues estimation in Guangdong province, China [127]. The efficiency for estimating grassland productivity showed that the C-Fix, a Monteith type parametric model, performed better than the BIOME-BGC model [128].

Besides, operational monitoring of the satellite-borne MODIS GPP/NPP products at the global scale are freely available now. The algorithm has fully considered the potential differences in light use efficiency affected by respiration cost and climatic factors among different vegetation types. The latest MOD17 products have good quality because the contaminated MODIS fPAR/LAI inputs to the MOD17 algorithm have been cleaned [129]. These products are good at studying general trends in the magnitude of NPP and GPP linked with local climate and land use. But both of them have a tendency to be high at low productivity sites and to be underestimated at high productivity sites [130,131]. It means that many results with these products may not always be dependable [132].

3.3.3. The main constraint of LUE model and the prospect

The definition of LUEmax (maximum LUE) can be theoretically considered as the canopy photosynthesis capacity or maximum conversion rate of absorbed photosynthesis capacity or maximum conversion rate of APAR into biomass under optimal environmental conditions. It is more efficient to use a satellite-based LUE model to estimate vegetation productivity. However, a maximum LUE, the results of environmental stresses such as light intensity, temperature, water, and nutrients, is often used as actual LUE and is a constant for a specific crop in estimating vegetation productivity, resulting in large errors [133–135]. In practice, LUEmax varies greatly with different crop varieties and is also affected by other factors such as spatial scale [136,137].

NPP can be used to measure the consequences caused by climate change and human activities on biomass accumulation and energy fluxes in natural ecosystems and managed lands [117,138,139] and the effects are complex for variant crops at different regions. Usually, it often leads to the poor estimation of ANPP (above-ground net primary productivity) in areas where herbaceous and woody plant types are spatially intermingled [140,141].

Actual LUEmax derived from RS data can significantly improve biomass estimation accuracy with explicit spatial-distribution [142]. Besides, the newly emerging satellite retrieval, solar-induced chlorophyll fluorescence (SIF), provides a direct, accurate and time-resolved measurement related to crop photosynthetic activity. The SIF-based approach accounts for photosynthetic pathways, so it can provide more reliable projections of vegetation productivity. Enhanced observational capabilities for SIF also help improve the mechanistic understanding of crop yield, especially in fragmented agricultural areas in response to climate variability and changes [143–145].

3.4. Crop height –based estimation method

In agriculture, the spatial distribution of crop height is valuable for biomass estimation and can improve field-work efficiency in terms of fertilization, pesticide application, irrigation, etc. Some factors such as cost and efficiency, flexibility and temporal-spatial resolution involved in measurements often limit the application of existing methods for capturing crop height [6,146,147].

3.4.1. Approaches to derive crop height

Approaches for deriving crop height vary widely [148]. Light detection and ranging (LiDAR) instruments utilize their own active light source to collect 3D geodata of surface objects at a rate of up to one million survey points per second. The laser beams can penetrate vegetation and measure the terrain without considering vegetation saturation even at very high biomass levels. Accordingly, physical proxies of plant biomass such as crop height, volume, and LAI can be derived [149–157], which is particularly applicable in energy crops. 3D geometry information from a high-resolution digital camera loaded on an unmanned aerial vehicle (UAV or unmanned aerial systems) can also be used for a crop surface model (CSM) [158,159].

When considering the application for small farmland, suitable data collection platforms can be ground-based like terrestrial laser scanners (TLS) [153,160,161] or airborne like UAVs [146,162]. The advantage of airborne laser scanning is its perspective close to nadir with minimum occlusion of the terrain by plants, but the weakness is its poor temporal and spatial resolution. To TLS data, the marked features are high-spatial resolution and accuracy of the point clouds. When deriving crop heights for a small field, one autonomously operating terrestrial laser scanning (ATLS) with an angular resolution of 8 mrad is enough [163]. A correlation between plant height and rice biomass with multitemporal CSMs based on TLS measurements was strong. The transferability of the established biomass regression model from a small-scale field experiment to larger-scale farmland is practicable [160]. However, the weakness of static terrestrial laser scanning is that it cannot eliminate occlusion of the terrain by vegetation and the data can contain unfavourable scanning geometries [163].

With the development of high-resolution digital cameras, RGB aerial imagery with cm-level spatial resolution can be easily obtained. A slightly higher correlation between yield and the combination of 3D CSMs and the VI information was found by using UAV-based CSMs and RGB-based VI information for early-to mid-season corn growth stages [164]. It is a feasible method to predict mid-season corn yield with

combined spectral and spatial modeling on the basis of aerial images and CSMs. Different growth stages can be obtained more accurate with a simple method for biomass estimation based on the plant height from CSMs [162]. Bendig et al. [165] assessed the spatial variability of crop height for both the field and plot scale and found that it is workable with the very high-spatial resolution data from the UAV for biomass prediction at a summer barley experiment compared to the VIs in the visible and near-infrared region. With UAV flight campaigns, the crop height changes and the calculation of growth rate can be recorded throughout the season [166].

Highly detailed point clouds data can be produced with the two methods, the UAV-based CSM and the TLS-based CSM. UAVs offers a fast, inexpensive and highly flexible data collection method for covering larger areas easily. However, data provided by UAVs might be less accurate, for example, the crop height derived from UAV is generally lower than the TLS-derived from early-to late-growth stage. Nevertheless, on the other side, the coefficient of variation is higher than in the TLS dataset [167]. To some extent, these two methods may be complementary. For example, the UAV approach can improve the occlusion effects of TLS [168]. Moreover, the main constraint of crop height measurements are the lodging cultivars in the later growth stages. Lodging leads to a lower average crop height than normal and so causes a poor relationship between biomass and plant heights [162].

3.4.2. Limitations of crop height information and the strength in future

Regarding the methods proposed for extracting crop height accurately, multiple factors including crop variety, growth period, and farmland management practices can affect the crop height, which ultimately limits the corresponding application. Particularly, one limitation is that the survey cannot be done on rainy days so rain often reduces the temporal resolution.

The time- and cost-efficient tools offered by working low-cost 3D cameras on farm machinery or on autonomous platforms can directly capture the spatial distribution of crop height in the field. Such information can help farmers to increase agricultural efficiency and productivity [169]. The practicability of ATLS, a static low-cost sensor, is its capability to cover the most key parts of a crop stand and so a network of ATLS can monitor larger and specific areas effectively [163]. Moreover, it is simple and cost-effective to collect RGB- imagery using UAV and to calculate RGB VI, which will be forthright suitable for farmers or unspecialized service providers [170,171].

The estimation method based on crop height is simple and cost-effective. But the robustness and applicability needs further improvement with multiple-year datasets during the growing stage of different cultivated varieties. Multi-source data from other imaging instruments such as multi-spectral, hyper-spectral and thermal cameras will play a complementary role in its improvement [165,172–177]. It will be a good chance to finish collecting a complete set of crop phenotypic indices at certain spatial- and temporal-scale, which is usually unavailable to plant scientists.

3.5. Crop growth model based estimation method with RS information

Knowledge about crop development is the foundation of optimized and efficient crop management. Crop growth models (CGMs) can simulate physical processes of crops under different environmental and management conditions. In this regard, these models are considered as a valuable tool to assess crop growing conditions and have the potential to support management decisions over large areas. Most CGMs e.g. DSSAT, STICS, and WOFOST are developed on similar radiation use efficiency approaches to simulate crop phenology and can forecast crop yield more accurate [178]. Generally, CGMs apply deterministic modeling strategies [179]. For field scale, such deterministic CGMs need a reasonable amount of input parameters concerning the nature of soil, climatic variables, crop management information, and agrotype. In fact, the shortage of the input parameters often constrains the CGMs performance. When applying CGMs over large areas, there is a great uncertainty. The integration of crop models and RS data is beneficial to the obtaining of crop growth information and crop yield by data assimilation (DA) method in a vast area (Fig. 3).

3.5.1. The integration of CGMs with RS data by data assimilation

Data assimilation is a process-based model and can estimate an unknown probability density function recursively over time. DA method can make the best use of earth observations e.g. measurements or remote sensing and thus advance the simulation skill. Biophysical and biochemical parameters e.g. LAI and leaf chlorophyll content from satellite images help improve the conditions of poor parameterization of CGMs [180]. The winter wheat biomass and yield were estimated more accurate by using the AquaCrop model with RS information [181]. As a combination of a probabilistic method and sequential DA, the Ensemble Kalman filter (EnKF) made crop models particularly useful. In addition, many crop models for implementation in the EnKF had an applicative structure, which often led to a relatively small model state vector [182]. By assimilating RapidEye data into APSIM, a deterministic CGM, the maize biomass prediction was optimized. The accuracy of biomass predictions for most maize fields with DA had an improvement of up to 15%. More detailed spatial variability of the biomass production was shown [183].

The dynamics simulation of certain crop by assimilating RS data into a CGM can be made better for site-specific farming. The corresponding results verified the temporal dynamics of the simulations and

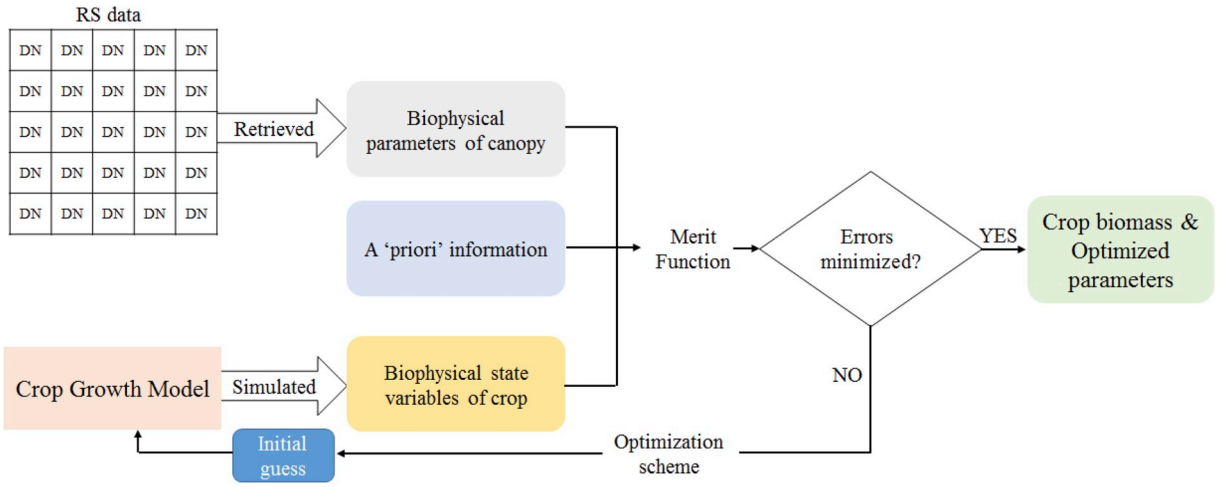

Fig. 3. A diagram of data assimilation strategy based on crop growth model and RS data.

the average correlation coefficient was 0.93 while average RMSE was 1.15 t ha^{-1} [184]. The assimilation of time-series of LAI derived from COSMO-SkyMed SAR images in AQUATER model led to significant improvements in forecasting the sugar beet and tomato yield, whereas the improvements were marginal for wheat yield over the Capitanata plain [185]. Assimilating biophysical parameters from RS data into crop models helps reduce uncertainties related to model inputs and improves the yield estimation [186]. Using a crop model-assimilated with EnKF based on RS data is useful for simulating crop growth and can help analysts evaluate the quality of RS data and crop model in estimating crop yield [187].

The link between crop models and RS data is particularly essential to improve the accuracy of crop models in estimating crop productivity [188,189]. Overall, a method that integrates RS information into CGMs is very useful for crop growth monitoring and crop biomass estimation.

3.5.2. Future prospects for CGMs

For only canopy state variables cannot improve energy crops management strategies, the most promising approach lies in the possibility of assimilating state variables from RS data into models. However, CGMs are generally deterministic unlike probabilistic models used in the fields of oceanography, meteorology and land surface hydrology, where advanced algorithms for sequential DA such as nudging and variational methods have been developed. It is still difficult to assimilate RS data into a CGM. Therefore, information on uncertainties of the model states, crucial for a successful application of most sequential DA algorithms, will not be provided by crop models during simulation. Even though crop biomass can be effectively estimated through assimilating RS information into crop models [190–194], an increasing number of RS data and more complex DA strategies require strong computing capability [182,188,189]. Moreover, the absence of real-time RS observations often makes it difficult to carry out successful assimilation of crop biomass [195,196]. Combining optical RS data with SAR data is a way to avoid missing the observations at critical growth stages, as the integration of these two data sources can exploit backscatter information pertinent to crop biophysical properties.

The advent of latest instruments characterized by high spatial, spectral and temporal resolution provides such a unique chance to overcome current limitations of point-based CGM approaches in heterogeneous agricultural regions. The within-field yield variability can be reproduced properly for precision energy crop management through data assimilation [197–200].

3.6. Challenges and opportunities for estimating energy crop biomass

The rapid development of RS technology has proposed some new satellite programs such as ICESat2 in the United States, BIOMASS satellite program by the ESA and ALOS PALSAR2 from Japan, providing a new platform for energy crop research with more reliable RS data. Simultaneously, the application of UAV and terrestrial 3D laser scanners and their combination with satellite RS technology improve the accuracy of energy crop biomass estimation. In addition, the capabilities to extract energy crop biophysical and biochemical parameters develop fast. In general, challenges and opportunities for energy crop biomass estimation based on RS information can be outlined as follows.

The good understanding between surface reflectance and vegetation characteristics makes optical sensors used widely. But the accuracy is not high enough due to many limiting factors. To microwave RS in estimating biomass, the application of fully polarimetric SAR sensors with very high resolution may establish a better relationship between radar backscatter and crop biophysical properties. The RS-based approaches evolve with high-quality RS data, and further work should be done on how to let the farming community learn these benefits and opportunities. Crop classification can be improved with optimal hypertemporal time series at minimum computational load, especially when rapid or remarkable changes in crop phenology exist in the growing period.

The NPP models should be further optimized. The potential is limited due to the models' complexity and scale conversion. Therefore, the reasonable simplification of the estimation models based on NPP is imperative. The extraction methods for RS information should be improved. Furthermore, different spatial scales often cause concern because different biodiversity information can be explored across various scales with different remotely sensed data.

The potential for biomass estimation based on crop height will be more important in the future research. The crop height information mainly come from UAV and terrestrial 3D laser scanning. Satellite RS data should be introduced so as to estimate energy crop biomass in larger regions. Meanwhile, the relationship between the factors affecting crop height and biomass needs better understanding for reducing transmission errors in the estimating process.

Estimating crop biomass by assimilating CGMs and RS information is promising, taking the physiological and ecological processes of crops into account. Increasing usage of real-time RS data will allow us to describe the growth of crops quantitatively and stimulate eco-physiological process more accurately in the future. Moreover, DA methods allow us to assimilate a variety of data with different spatiotemporal resolutions and measure error information, thereby improving simulation accuracy.

Crosschecking methods among different models and among multiple sources of data are also an option to help improve the accuracy of biomass estimations.

4. Conclusions

At present, the most popular method for estimating energy crop biomass is to perform a statistical analysis with traditional optical data. Though there are many shortcomings in the existing methods, it is an inevitable trend to use RS data to inform energy crop biomass estimation models. With the use of macroscopic and real-time RS information, those models can accurately reflect the overall condition of energy crops based on information about physiological and ecological mechanisms.

From traditional optical RS to microwaves, lasers to hyperspectral RS, continuous spectral information and finer spectral information can be derived. In the future, efforts should be made to model mechanism for energy crop biomass estimation with more reliable growth and development process.

Declarations of interest

None.

Acknowledgments

This research is supported by the National Social Science Fund of China (No. 14BJY064), the National Natural Science Foundation of China (No. 41701634) and the Nantong Key Laboratory Project (CP12016005). Special thanks to Mrs. Julie Watson and Dr. Wentao Ye for their continuous valuable suggestions and moral support. Deep gratitude will be for literature cited in this article.

References

[1] H. Yamamoto, Y. Matsumura, S. Sawayama, Evaluation of supply potential of energy crops in Japan considering cases of improvement of crop productivity, Biomass Bioenergy 29 (2005) 355–359.
[2] G. Berndes, M. Hoogwijk, R. van den Broek, The contribution of biomass in the future global energy supply: a review of 17 studies, Biomass Bioenergy 25 (2003) 1–28.
[3] T. Gomiero, M.G. Paoletti, D. Pimentel, Biofuels: efficiency, ethics, and limits to human appropriation of ecosystem services, J. Agric. Environ. Ethics 23 (2010) 403–434.
[4] M. Ostwald, A. Jonsson, V. Wibeck, T. Asplund, Mapping energy crop cultivation

and identifying motivational factors among Swedish farmers, Biomass Bioenergy 50 (2013) 25–34.
[5] S. Landström, L. Lomakka, S. Andersson, Harvest in spring improves yield and quality of reed canary grass as a bioenergy crop, Biomass Bioenergy 11 (1996) 333–341.
[6] R.N. Lati, S. Filin, H. Eizenberg, Estimating plant growth parameters using an energy minimization-based stereovision model, Comput. Electron. Agric. 98 (2013) 260–271.
[7] M.B. Villamil, M. Alexander, A.H. Silvis, M.E. Gray, Producer perceptions and information needs regarding their adoption of bioenergy crops, Renew. Sustain. Energy Rev. 16 (2012) 3604–3612.
[8] M.E. Goerndt, B.T. Wilson, F.X. Aguilar, Comparison of small area estimation methods applied to biopower feedstock supply in the Northern U.S. region, Biomass Bioenergy 121 (2019) 64–77.
[9] S.S. Panda, D.P. Ames, S. Panigrahi, Application of vegetation indices for agricultural crop yield prediction using neural network techniques, Rem. Sens. 2 (2010) 673–696.
[10] K. Calvert, Geomatics and bioenergy feasibility assessments: taking stock and looking forward, Renew. Sustain. Energy Rev. 15 (2011) 1117–1124.
[11] K. Calvert, J.M. Pearce, W.E. Mabee, Toward renewable energy geo-information infrastructures: applications of GIScience and remote sensing that build institutional capacity, Renew. Sustain. Energy Rev. 18 (2013) 416–429.
[12] D. Haboudane, N. Tremblay, J.R. Miller, P. Vigneault, Remote estimation of crop chlorophyll content using spectral indices derived from hyperspectral data, IEEE Trans. Geosci. Remote Sens. 46 (2008) 423–437.
[13] T. Hammar, J. Stendahl, C. Sundberg, H. Holmström, P.-A. Hansson, Climate impact and energy efficiency of woody bioenergy systems from a landscape perspective, Biomass Bioenergy 120 (2019) 189–199.
[14] T. Ahamed, L. Tian, N. Ryozo, T. Takigawa, Remote Sensing Applications of Estimating Biomass for Energy Crops: Development of Ground-Based Sensing Systems, Nova Science Publishers, Inc., 2013.
[15] S. Moulin, A. Bondeau, R. Delecolle, Combining agricultural crop models and satellite observations: from field to regional scales, Int. J. Remote Sens. 19 (1998) 1021–1036.
[16] A.O. Onojeghuo, G.A. Blackburn, J. Huang, D. Kindred, W. Huang, Applications of satellite 'hyper-sensing' in Chinese agriculture: challenges and opportunities, Int. J. Appl. Earth Obs. Geoinf. 64 (2018) 62–86.
[17] I. Ali, F. Cawkwell, E. Dwyer, B. Barrett, S. Green, Satellite remote sensing of grasslands: from observation to management, J. Plant Ecol. 9 (2016) 649–671.
[18] T. Ahamed, L. Tian, Y. Zhang, K.C. Ting, A review of remote sensing methods for biomass feedstock production, Biomass Bioenergy 35 (2011) 2455–2469.
[19] G.A. Blackburn, C.M. Steele, Towards the remote sensing of matorral vegetation physiology : relationships between spectral reflectance, pigment, and biophysical characteristics of semiarid bushland canopies, Remote Sens. Environ. 70 (1999) 278–292.
[20] E. Boegh, H. Soegaard, N. Broge, C.B. Hasager, N.O. Jensen, K. Schelde, A. Thomsen, Airborne multispectral data for quantifying leaf area index, nitrogen concentration, and photosynthetic efficiency in agriculture, Remote Sens. Environ. 81 (2002) 179–193.
[21] L. Di, D.C. Rundquist, L. Han, Modelling relationships between NDVI and precipitation during vegetative growth cycles, Int. J. Remote Sens. 15 (1994) 2121–2136.
[22] C.D. Elvidge, Z. Chen, Comparison of broad-band and narrow-band red and near-infrared vegetation indices, Remote Sens. Environ. 54 (1995) 38–48.
[23] X. Gao, A.R. Huete, W. Ni, T. Miura, Optical–biophysical relationships of vegetation spectra without background contamination, Remote Sens. Environ. 74 (2000) 609–620.
[24] A.A. Gitelson, A. Viña, T.J. Arkebauer, D.C. Rundquist, G.P. Keydan, B. Leavitt, Remote estimation of leaf area index and green leaf biomass in maize canopies, Geophys. Res. Lett. 30 (2003) 52–55.
[25] Y.M. Govaerts, M.M. Verstraete, B. Pinty, N. Gobron, Designing optimal spectral indices: a feasibility and proof of concept study, Int. J. Remote Sens. 20 (1999) 1853–1873.
[26] R.D. Jackson, A.R. Huete, Interpreting vegetation indices, Prev. Vet. Med. 11 (1991) 185–200.
[27] J.R. Jensen, Remote Sensing of the Environment: an Earth Resource Perspective, second ed., Pearson Prentice Hall, Upper Saddle River, NJ, USA, 2007.
[28] R.B. Myneni, F.G. Hall, P.J. Sellers, A. Marshak, The interpretation of spectral vegetation indexes, IEEE Trans. Geosci. Remote Sens. 33 (1995) 481–486.
[29] R.A. Schowengerdt, Techniques for Image Processing and Classification in Remote Sensing, Academic Press, New York, 1983.
[30] C.J. Tucker, Red and photographic infrared linear combinations for monitoring vegetation, Remote Sens. Environ. 8 (1979) 127–150.
[31] N.H. Broge, J.V. Mortensen, Deriving green crop area index and canopy chlorophyll density of winter wheat from spectral reflectance data, Remote Sens. Environ. 81 (2002) 45–57.
[32] A. Nguy-Robertson, A. Gitelson, Y. Peng, A. Viña, T. Arkebauer, D. Rundquist, Green leaf area index estimation in maize and soybean: combining vegetation indices to achieve maximal sensitivity, Agron. J. 104 (2012) 1336–1347.
[33] C. Wu, Z. Niu, Q. Tang, W. Huang, Estimating chlorophyll content from hyperspectral vegetation indices: modeling and validation, Agric. For. Meteorol. 148 (2008) 1230–1241.
[34] Q. Xie, W. Huang, D. Liang, P. Chen, C. Wu, G. Yang, J. Zhang, L. Huang, D. Zhang, Leaf area index estimation using vegetation indices derived from airborne hyperspectral images in winter wheat, IEEE J. Sel. Topics. Appl. Earth. Observ Remote. Sens. 7 (2014) 3586–3594.
[35] S.W. Todd, R.M. Hoffer, D.G. Milchunas, Biomass estimation on grazed and ungrazed rangelands using spectral indices, Int. J. Remote Sens. 19 (1998) 427–438.
[36] W. Collins, Remote sensing of crop type and maturity, Photogramm. Eng. Rem. Sens. 44 (1978) 43–55.
[37] D.N.H. Horler, M. Dockray, J. Barber, The red edge of plant leaf reflectance, Int. J. Remote Sens. 4 (1983) 273–288.
[38] O. Mutanga, A.K. Skidmore, Narrow band vegetation indices overcome the saturation problem in biomass estimation, Int. J. Remote Sens. 25 (2004) 3999–4014.
[39] N.S. Lucas, P.J. Curran, S.E. Plummer, F.M. Danson, Estimating the stem carbon production of a coniferous forest using an ecosystem simulation model driven by the remotely sensed red edge, Int. J. Remote Sens. 21 (2000) 619–631.
[40] J.G.P.W. Clevers, G.W.A.M.v.d. Heijden, S. Verzakov, M.E. Schaepman, Estimating grassland biomass using SVM band shaving of hyperspectral data, Photogramm. Eng. Rem. Sens. 73 (2007) 1141–1148.
[41] M. Sibanda, O. Mutanga, M. Rouget, Comparing the spectral settings of the new generation broad and narrow band sensors in estimating biomass of native grasses grown under different management practices, GIsci. Remote. Sens. 53 (2016) 614–633.
[42] P. Gong, R. Pu, G.S. Biging, M.R. Larrieu, Estimation of forest leaf area index using vegetation indices derived from hyperion hyperspectral data, IEEE Trans. Geosci. Remote Sens. 41 (2003) 1355–1362.
[43] T.F. Porter, C. Chen, J.A. Long, R.L. Lawrence, B.F. Sowell, Estimating biomass on CRP pastureland: a comparison of remote sensing techniques, Biomass Bioenergy 66 (2014) 268–274.
[44] L. Zeng, C. Chen, Using remote sensing to estimate forage biomass and nutrient contents at different growth stages, Biomass Bioenergy 115 (2018) 74–81.
[45] C.F. Jordan, Derivation of leaf-area index from quality of light on the forest floor, Ecology 50 (1969) 663–666.
[46] J.W. Rouse Jr., R.H. Haas, J.A. Schell, D.W. Deering, Monitoring vegetation systems in the great plains with ERTS, NASA. Goddard Space Flight Center 3d ERTS-1 Symp 1 (1974) 309–317.
[47] A.R. Huete, H.Q. Liu, K. Batchily, W. van Leeuwen, A comparison of vegetation indices over a global set of TM images for EOS-MODIS, Remote Sens. Environ. 59 (1997) 440-445-451.
[48] A.A. Gitelson, Y.J. Kaufman, M.N. Merzlyak, Use of a green channel in remote sensing of global vegetation from EOS-MODIS, Remote Sens. Environ. 58 (1996) 289–298.
[49] A.A. Gitelson, Wide dynamic range vegetation index for remote quantification of biophysical characteristics of vegetation, J. Plant Physiol. 161 (2004) 165–173.
[50] A.A. Gitelson, A. Viña, V. Ciganda, D.C. Rundquist, T.J. Arkebauer, Remote estimation of canopy chlorophyll content in crops, Geophys. Res. Lett. 32 (2005) L08403.08401-L08403.08404.
[51] A.A. Gitelson, Y. Gritz, M.N. Merzlyak, Relationships between leaf chlorophyll content and spectral reflectance and algorithms for non-destructive chlorophyll assessment in higher plant leaves, J. Plant Physiol. 160 (2003) 271–282.
[52] A.A. Gitelson, S.B. Verma, A. Viña, D.C. Rundquist, G.P. Keydan, B. Leavitt, T.J. Arkebauer, G.G. Burba, A.E. Suyker, Novel technique for remote estimation of CO2 flux in maize, Geophys. Res. Lett. 30 (2003) 1486.
[53] J. Dash, P.J. Curran, The MERIS terrestrial chlorophyll index, Int. J. Remote Sens. 25 (2004) 5403–5413.
[54] A.R. Huete, A soil-adjusted vegetation index (SAVI), Remote Sens. Environ. 25 (1988) 295–309.
[55] J. Qi, A. Chehbouni, A.R. Huete, Y.H. Kerr, S. Sorooshian, A modified soil adjusted vegetation index, Remote Sens. Environ. 48 (1994) 119–126.
[56] J.-L. Roujean, B. F, Estimating PAR absorbed by vegetation from bidirectional reflectance measurements, Remote Sens. Environ. 51 (1995) 375–384.
[57] G.L. Anderson, Evaluating Landsat Thematic Mapper derived vegetation indices for estimating above-ground biomass on semiarid rangelands, Remote Sens. Environ. 45 (1993) 165–175.
[58] B.K. Wylie, J.A. Harrington, S.D. Prince, I. Demda, Satellite and ground-based pasture production assessment in Niger: 1986-1988, Int. J. Remote Sens. 12 (1991) 1281–1300.
[59] E. Lokupitiya, M. Lefsky, K. Paustian, Use of AVHRR NDVI time series and ground-based surveys for estimating county-level crop biomass, Int. J. Remote Sens. 31 (2010) 141–158.
[60] M. Claverie, V. Demarez, B. Duchemin, O. Hagolle, D. Ducrot, C. Marais-Sicre, J.-F. Dejoux, M. Huc, P. Keravec, P. Béziat, R. Fieuzal, E. Ceschia, G. Dedieu, Maize and sunflower biomass estimation in southwest France using high spatial and temporal resolution remote sensing data, Remote Sens. Environ. 124 (2012) 844–857.
[61] C. Liao, J. Wang, T. Dong, J. Shang, J. Liu, Y. Song, Using spatio-temporal fusion of Landsat-8 and MODIS data to derive phenology, biomass and yield estimates for corn and soybean, Sci. Total Environ. 650 (2019) 1707–1721.
[62] J. Wang, J. Huang, P. Gao, C. Wei, L. Mansaray, Dynamic mapping of rice growth parameters using HJ-1 CCD time series data, Rem. Sens. 8 (2016) 931.
[63] S. Stagakis, N. Markos, O. Sykioti, A. Kyparissis, Monitoring canopy biophysical and biochemical parameters in ecosystem scale using satellite hyperspectral imagery: an application on a Phlomis fruticosa Mediterranean ecosystem using multiangular CHRIS/PROBA observations, Remote Sens. Environ. 114 (2010) 977–994.
[64] A. Viña, A.A. Gitelson, A.L. Nguy-Robertson, Y. Peng, Comparison of different vegetation indices for the remote assessment of green leaf area index of crops, Remote Sens. Environ. 115 (2011) 3468–3478.
[65] D. Wehlage, J. Gamon, D. Thayer, D. Hildebrand, Interannual variability in dry mixed-grass prairie yield: a comparison of MODIS, SPOT, and field measurements,

Rem. Sens. 8 (2016) 872–890.
[66] P.F. Chen, T. Nicolas, J.H. Wang, V. Philippe, W.J. Huang, New index for crop canopy fresh biomass estimation, Spectrosc. Spectr. Anal. 30 (2010) 512–517.
[67] X.H. Hou, Z. Niu, N. Huang, S.G. Xu, The hyperspectral remote sensing estimation models of total biomass and true LAI of wheat, Remote Sens. Land Resour. 24 (2012) 30–35.
[68] P.S. Thenkabail, R.B. Smith, E. De Pauw, Hyperspectral vegetation indices and their relationships with agricultural crop characteristics, Remote Sens. Environ. 71 (2000) 158–182.
[69] K. Song, D. Liu, Z. Wang, D. Lu, B. Zhang, C. Ren, J. Du, Corn chlorophyll-a concentration and LAI estimation models based on wavelet transformed canopy hyperspectral reflectance, Syst. Sci. Compreh. Stud. Agric. 27 (2011) 154–160.
[70] A. Kross, H. McNairn, D. Lapen, M. Sunohara, C. Champagne, Assessment of RapidEye vegetation indices for estimation of leaf area index and biomass in corn and soybean crops, Int. J. Appl. Earth Obs. Geoinf. 34 (2015) 235–248.
[71] X. Wang, J. Huang, Y. Li, R. Wang, Study on hyperspectral remote sensing estimation models for the ground fresh biomass of rice, Acta Agron. Sin. 29 (2003) 815–821.
[72] Y. Mo, M.S. Kearney, J.C.A. Riter, F. Zhao, D.R. Tilley, Assessing biomass of diverse coastal marsh ecosystems using statistical and machine learning models, Int. J. Appl. Earth Obs. Geoinf. 68 (2018) 189–201.
[73] S. Ullah, Y. Si, M. Schlerf, A.K. Skidmore, M. Shafique, I.A. Iqbal, Estimation of grassland biomass and nitrogen using MERIS data, Int. J. Appl. Earth Obs. Geoinf. 19 (2012) 196–204.
[74] H. Meyer, L.W. Lehnert, Y. Wang, C. Reudenbach, T. Nauss, J. Bendix, From local spectral measurements to maps of vegetation cover and biomass on the Qinghai-Tibet-Plateau: do we need hyperspectral information? Int. J. Appl. Earth Obs. Geoinf. 55 (2017) 21–31.
[75] J.-P. Lagouarde, F. Jacob, X.F. Gu, A. Olioso, J.-M. Bonnefond, Y. Kerr, K.J. Mcaneney, M. Irvine, Spatialization of sensible heat flux over a heterogeneous landscape, Agronomie 22 (2002) 627–633.
[76] C. Sannier, R.E. McRoberts, L.-V. Fichet, E.M.K. Makaga, Using the regression estimator with Landsat data to estimate proportion forest cover and net proportion deforestation in Gabon, Remote Sens. Environ. 151 (2014) 138–148.
[77] M.C. Hansen, P.V. Potapov, R. Moore, M. Hancher, S.A. Turubanova, A. Tyukavina, D. Thau, S.V. Stehman, S.J. Goetz, T.R. Loveland, A. Kommareddy, A. Egorov, L. Chini, C.O. Justice, J.R.G. Townshend, High-resolution global maps of 21st-century forest cover change, Science 342 (2013) 850–853.
[78] J.Q. Chambers, G.P. Asner, D.C. Morton, L.O. Anderson, S.S. Saatchi, F.D. Espirito-Santo, M. Palace, C. Souza Jr., Regional ecosystem structure and function: ecological insights from remote sensing of tropical forests, Trends Ecol. Evol. 22 (2007) 414–423.
[79] G.P. Asner, Cloud cover in Landsat observations of the Brazilian Amazon, Int. J. Remote Sens. 22 (2001) 3855–3862.
[80] I. Becker-Reshef, E. Vermote, M. Lindeman, C. Justice, A generalized regression-based model for forecasting winter wheat yields in Kansas and Ukraine using MODIS data, Remote Sens. Environ. 114 (2010) 1312–1323.
[81] K. Zhao, D. Valle, S. Popescu, X. Zhang, B. Mallick, Hyperspectral remote sensing of plant biochemistry using Bayesian model averaging with variable and band selection, Remote Sens. Environ. 132 (2013) 102–119.
[82] D. Lu, The potential and challenge of remote sensing-based biomass estimation, Int. J. Remote Sens. 27 (2006) 1297–1328.
[83] S. Tao, Q. Guo, B. Wu, L. Li, S. Wang, Z. Tang, B. Xue, J. Liu, J. Fang, Spatial scale and pattern dependences of aboveground biomass estimation from satellite images: a case study of the Sierra National Forest, California, Landsc. Ecol. 31 (2016) 1711–1723.
[84] J.M. Chen, Spatial scaling of a remotely sensed surface parameter by contexture, Remote Sens. Environ. 69 (1999) 30–42.
[85] M. Hajj, N. Baghdadi, G. Belaud, M. Zribi, B. Cheviron, D. Courault, O. Hagolle, F. Charron, Irrigated grassland monitoring using a time series of TerraSAR-X and COSMO-SkyMed X-band SAR data, Rem. Sens. 6 (2014) 10002–10032.
[86] B. Barrett, I. Nitze, S. Green, F. Cawkwell, Assessment of multi-temporal, multi-sensor radar and ancillary spatial data for grasslands monitoring in Ireland using machine learning approaches, Remote Sens. Environ. 152 (2014) 109–124.
[87] T. Gao, B. Xu, X. Yang, Y. Jin, H. Ma, J. Li, H. Yu, Using MODIS time series data to estimate aboveground biomass and its spatio-temporal variation in Inner Mongolia's grassland between 2001 and 2011, Int. J. Remote Sens. 34 (2013) 7796–7810.
[88] Y. Inoue, T. Kurosu, H. Maeno, S. Uratsuka, T. Kozu, K. Dabrowska-Zielinska, J. Qi, Season-long daily measurements of multifrequency (Ka, Ku, X, C, and L) and full-polarization backscatter signatures over paddy rice field and their relationship with biological variables, Remote Sens. Environ. 81 (2002) 194–204.
[89] A. Metz, A. Schmitt, T. Esch, P. Reinartz, S. Klonus, M. Ehlers, Synergetic Use of TerraSAR-X and Radarsat-2 Time Series Data for Identification and Characterization of Grassland Types - a Case Study in Southern Bavaria, Germany, IGARSS, 2012 IEEE International, 2012, pp. 3560–3563.
[90] K. Voormansik, T. Jagdhuber, A. Olesk, I. Hajnsek, K.P. Papathanassiou, Towards a detection of grassland cutting practices with dual polarimetric TerraSAR-X data, Int. J. Remote Sens. 34 (2013) 8081–8103.
[91] J.R. Buckley, A.M. Smith, Monitoring Grasslands with Radarsat 2 Quad-Pol Imagery, IGARSS, 2010 IEEE International, 2010, pp. 3090–3093.
[92] S. Mermoz, M. Réjou-Méchain, L. Villard, T. Le Toan, V. Rossi, S. Gourlet-Fleury, Decrease of L-band SAR backscatter with biomass of dense forests, Remote Sens. Environ. 159 (2015) 307–317.
[93] M. Hosseini, H. McNairn, A. Merzouki, A. Pacheco, Estimation of Leaf Area Index (LAI) in corn and soybeans using multi-polarization C- and L-band radar data, Remote Sens. Environ. 170 (2015) 77–89.
[94] M. Pichierri, I. Hajnsek, S. Zwieback, B. Rabus, On the potential of Polarimetric SAR Interferometry to characterize the biomass, moisture and structure of agricultural crops at L-, C- and X-Bands, Remote Sens. Environ. 204 (2018) 596–616.
[95] M. Chakraborty, K.R. Manjunath, S. Panigrahy, N. Kundu, J.S. Parihar, Rice crop parameter retrieval using multi-temporal, multi-incidence angle Radarsat SAR data, ISPRS J. Photogrammetry Remote Sens. 59 (2005) 310–322.
[96] Z. Yang, K. Li, Y. Shao, B. Brisco, L. Liu, Estimation of paddy rice variables with a modified water cloud model and improved polarimetric decomposition using multi-temporal RADARSAT-2 images, Rem. Sens. 8 (2016) 878.
[97] Y. Inoue, E. Sakaiya, C. Wang, Potential of X-band images from high-resolution satellite SAR sensors to assess growth and yield in paddy rice, Rem. Sens. 6 (2014) 5995–6019.
[98] G. Wiseman, H. McNairn, S. Homayouni, J. Shang, RADARSAT-2 polarimetric SAR response to crop biomass for agricultural production monitoring, IEEE J. Sel. Topics. Appl. Earth. Observ Remote. Sens. 7 (2014) 4461–4471.
[99] G. Macelloni, S. Paloscia, P. Pampaloni, F. Marliani, M. Gai, The relationship between the backscattering coefficient and the biomass of narrow and broad leaf crops, IEEE Trans. Geosci. Remote Sens. 39 (2001) 873–884.
[100] H. McNairn, B. Brisco, The application of C-band polarimetric SAR for agriculture: a review, Can. J. Remote Sens. 30 (2004) 525–542.
[101] Z. He, S. Li, Y. Wang, L. Dai, S. Lin, Monitoring rice phenology based on backscattering characteristics of multi-temporal RADARSAT-2 datasets, Rem. Sens. 10 (2018) 340.
[102] W. Koppe, M.L. Gnyp, S.D. Hennig, F. Li, Y. Miao, X. Chen, L. Jia, G. Bareth, Multi-temporal hyperspectral and radar remote sensing for estimating winter wheat biomass in the North China Plain, Photogramm. Fernerkund. Geoinf. 3 (2012) 281–298.
[103] M. Hosseini, H. McNairn, Using multi-polarization C- and L-band synthetic aperture radar to estimate biomass and soil moisture of wheat fields, Int. J. Appl. Earth Obs. Geoinf. 58 (2017) 50–64.
[104] A.G. Konings, M. Piles, N. Das, D. Entekhabi, L-band vegetation optical depth and effective scattering albedo estimation from SMAP, Remote Sens. Environ. 198 (2017) 460–470.
[105] A. Lopes, R. Touzi, E. Nezry, Adaptive speckle filters and scene heterogeneity, IEEE Trans. Geosci. Remote Sens. 28 (1990) 992–1000.
[106] M.S. Moran, Y. Inoue, E.M. Barnes, Opportunities and limitations for image-based remote sensing in precision crop management, Remote Sens. Environ. 61 (1997) 319–346.
[107] S. Quegan, J.J. Yu, Filtering of multichannel SAR images, IEEE Trans. Geosci. Remote Sens. 39 (2001) 2373–2379.
[108] Y. Maghsoudi, M.J. Collins, D. Leckie, Speckle reduction for the forest mapping analysis of multi-temporal Radarsat-1 images, Int. J. Remote Sens. 33 (2012) 1349–1359.
[109] I. Woodhouse, Introduction to Microwave Remote Sensing, CRC Press, Taylor & Francis Group, Boca Raton, FL, USA, 2005.
[110] L. Baldini, N. Roberto, E. Gorgucci, J. Fritz, V. Chandrasekar, Analysis of dual polarization images of precipitating clouds collected by the COSMO SkyMed constellation, Atmos. Res. 144 (2014) 21–37.
[111] A. Rosenqvist, M. Shimada, N. Ito, M. Watanabe, ALOS PALSAR: a Pathfinder mission for global-scale monitoring of the environment, IEEE Trans. Geosci. Remote Sens. 45 (2007) 3307–3316.
[112] N. Joshi, M. Baumann, A. Ehammer, R. Fensholt, K. Grogan, P. Hostert, M. Jepsen, T. Kuemmerle, P. Meyfroidt, E. Mitchard, J. Reiche, C. Ryan, B. Waske, A review of the application of optical and radar remote sensing data fusion to land use mapping and monitoring, Rem. Sens. 8 (2016) 70–92.
[113] R.H. Waring, W. J, J.E.R. H, M. L, R.K. Jon, W.J. F, O. Ram, F.S. E, Imaging radar for ecosystem studies, Bioscience 45 (1995) 715–723.
[114] D. Chi, H. Wang, X. Li, H. Liu, X. Li, Assessing the effects of grazing on variations of vegetation NPP in the Xilingol Grassland, China, using a grazing pressure index, Ecol. Indicat. 88 (2018) 372–383.
[115] G. Sun, M. Mu, Assessing the characteristics of net primary production due to future climate change and CO 2 under RCP4.5 in China, Ecol. Complex. 34 (2018) 58–68.
[116] M. Tum, J.N. Zeidler, K.P. Günther, T. Esch, Global NPP and straw bioenergy trends for 2000–2014, Biomass Bioenergy 90 (2016) 230–236.
[117] S. Gingrich, M. Niedertscheider, T. Kastner, H. Haberl, G. Cosor, F. Krausmann, T. Kuemmerle, D. Müller, A. Reith-Musel, M.R. Jepsen, A. Vadineanu, K.-H. Erb, Exploring long-term trends in land use change and aboveground human appropriation of net primary production in nine European countries, Land Use Pol. 47 (2015) 426–438.
[118] M.C. Reeves, M.A. L, K.E. Bagne, S.W. Running, Estimating climate change effects on net primary production of rangelands in the United States, Clim. Change (2014) 429–442.
[119] J. Zhan, N. Shi, S. He, Y. Lin, Factors and mechanism driving the land-use conversion in Jiangxi Province, J. Geogr. Sci. 20 (2010) 525–539.
[120] C.R. Schwalm, C.A. Williams, K. Schaefer, R. Anderson, M.A. Arain, I. Baker, A. Barr, T.A. Black, G. Chen, J.M. Chen, P. Ciais, K.J. Davis, A. Desai, M. Dietze, D. Dragoni, M.L. Fischer, L.B. Flanagan, R. Grant, L. Gu, D. Hollinger, R.C. Izaurralde, C. Kucharik, P. Lafleur, B.E. Law, L. Li, Z. Li, S. Liu, E. Lokupitiya, Y. Luo, S. Ma, H. Margolis, R. Matamala, H. McCaughey, R.K. Monson, W.C. Oechel, C. Peng, B. Poulter, D.T. Price, D.M. Riciutto, W. Riley, A.K. Sahoo, M. Sprintsin, J. Sun, H. Tian, C. Tonitto, H. Verbeeck, S.B. Verma, A model-data intercomparison of CO_2 exchange across North America: results from the North American Carbon Program site synthesis, J. Geophys. Res. 115 (2010) G00H05.01-G00H05.01-22.

[121] B. Yu, F. Chen, The global impact factors of net primary production in different land cover types from 2005 to 2011, SpringerPlus 5 (2016) 1235–1247.
[122] A.D. Friend, Terrestrial plant production and climate change, J. Exp. Bot. 61 (2010) 1293–1309.
[123] R. Frouin, R.T. Pinker, Estimating photosynthetically active radiation (PAR) at the earth's surface from satellite observations, Remote Sens. Environ. 51 (1995) 98–107.
[124] J.W. Seaquist, L. Olsson, Rapid estimation of photosynthetically active radiation over the west African Sahel using the pathfinder land data set, Int. J. Appl. Earth Obs. Geoinf. 1 (1999) 205–213.
[125] F. Tao, M. Yokozawa, Z. Zhang, Y. Xu, Y. Hayashi, Remote sensing of crop production in China by production efficiency models: models comparisons, estimates and uncertainties, Ecol. Model. 183 (2005) 385–396.
[126] S.I. Na, S.Y. Hong, Y.H. Kim, K.D. Lee, S.Y. Jang, Prediction of rice yield in Korea using paddy rice NPP index - application of MODIS data and CASA Model, Korean J. Remote Sens. 29 (2013) 461–476.
[127] F. Wang, X. Li, X. Shi, Estimation of cropland residue bioenergy using remote sensing: a case study of Guangdong province, J. Nat. Resour. 21 (2006) 870–878.
[128] F. Maselli, G. Argenti, M. Chiesi, L. Angeli, D. Papale, Simulation of grassland productivity by the combination of ground and satellite data, Agric. Ecosyst. Environ. 165 (2013) 163–172.
[129] S. Running, Q. Mu, M. Zhao, MYD17A3H MODIS/Aqua Net Primary Production Yearly L4 Global 500m SIN Grid V006, (2015).
[130] C.O. Justice, J.R.G. Townshend, V.E. F, E. Masuoka, R.E. Wolfe, W.N. Saleous, D.P. Roy, J.T. Morisette, An overview of MODIS Land data processing and product status, Remote Sens. Environ. 83 (2002) 3–15.
[131] D.P. Turner, W.D. Ritts, W.B. Cohen, S.T. Gower, S.W. Running, M. Zhao, M.H. Costa, A.A. Kirschbaum, J.M. Ham, S.R. Saleska, D.E. Ahl, Evaluation of MODIS NPP and GPP products across multiple biomes, Remote Sens. Environ. 102 (2006) 282–292.
[132] P. Propastin, M. Kappas, Modeling net ecosystem exchange for grassland in central Kazakhstan by combining remote sensing and field data, Rem. Sens. 1 (2009) 159–183.
[133] T. Hilker, N.C. Coops, M.A. Wulder, T.A. Black, R.D. Guy, The use of remote sensing in light use efficiency based models of gross primary production: a review of current status and future requirements, Sci. Total Environ. 404 (2008) 411–423.
[134] J.L. Monteith, Solar radiation and productivity in tropical ecosystems, J. Appl. Ecol. 9 (1972) 747–766.
[135] Z. Chao, P. Zhang, X. Wang, Impacts of urbanization on the net primary productivity and cultivated land change in Shandong province, China, J. Indian Soc. Rem. Sens. 46 (2018) 809–819.
[136] J. Morel, A. Bégué, P. Todoroff, J.-F. Martiné, V. Lebourgeois, M. Petit, Coupling a sugarcane crop model with the remotely sensed time series of fIPAR to optimise the yield estimation, Eur. J. Agron. 61 (2014) 60–68.
[137] Q. Xin, M. Broich, A.E. Suyker, L. Yu, P. Gong, Multi-scale evaluation of light use efficiency in MODIS gross primary productivity for croplands in the Midwestern United States, Agric. For. Meteorol. 201 (2015) 111–119.
[138] F. Krausmann, K.-H. Erb, S. Gingrich, H. Haberl, A. Bondeau, V. Gaube, C. Lauk, C. Plutzar, T.D. Searchinger, Global human appropriation of net primary production doubled in the 20th century, PANS (Pest. Artic. News Summ.) 110 (2013) 10324–10329.
[139] R.R. Nemani, C.D. Keeling, H. Hashimoto, W.M. Jolly, S.C. Piper, C.J. Tucker, R.B. Myneni, S.W. Running, Climate-driven increases in global terrestrial net primary production from 1982 to 1999, Science 300 (2003) 1560–1563.
[140] L.J. Blanco, J.M. Paruelo, M. Oesterheld, F.N. Biurrun, Spatial and temporal patterns of herbaceous primary production in semi-arid shrublands: a remote sensing approach, J. Veg. Sci. 27 (2016) 716–727.
[141] N. An, K.P. Price, J.M. Blair, Estimating above-ground net primary productivity of the tallgrass prairie ecosystem of the Central Great Plains using AVHRR NDVI, Int. J. Remote Sens. 34 (2013) 3717–3735.
[142] T. Dong, J. Liu, B. Qian, Q. Jing, H. Croft, J. Chen, J. Wang, T. Huffman, J. Shang, P. Chen, Deriving maximum light use efficiency from crop growth model and satellite data to improve crop biomass estimation, IEEE J. Sel. Topics. Appl. Earth Observ Remote. Sens. 10 (2017) 104–117.
[143] K. Guan, J.A. Berry, Y. Zhang, J. Joiner, L. Guanter, G. Badgley, D.B. Lobell, Improving the monitoring of crop productivity using spaceborne solar-induced fluorescence, Glob. Chang. Biol. 22 (2016) 716–726.
[144] L. Guanter, Y. Zhang, M. Jung, J. Joiner, M. Voigt, J.A. Berry, C. Frankenberg, A.R. Huete, P. Zarco-Tejada, J.E. Lee, M.S. Moran, G. Ponce-Campos, C. Beer, G. Camps-Valls, N. Buchmann, D. Gianelle, K. Klumpp, A. Cescatti, J.M. Baker, T.J. Griffis, Global and time-resolved monitoring of crop photosynthesis with chlorophyll fluorescence, Proc. Natl. Acad. Sci. Unit. States Am. 111 (2014) E1327–E1333.
[145] Y. Sun, C. Frankenberg, M. Jung, J. Joiner, L. Guanter, P. Köhler, T. Magney, Overview of solar-induced chlorophyll fluorescence (SIF) from the orbiting carbon observatory-2: retrieval, cross-mission comparison, and global monitoring for GPP, Remote Sens. Environ. 209 (2018) 808–823.
[146] J. Bendig, A. Bolten, G. Bareth, UAV-based imaging for multi-temporal, very high resolution crop surface models to monitor crop growth variability, Photogramm. Fernerkund. Geoinf. 6 (2013) 0551–0562.
[147] D. Hoffmeister, A. Bolten, C. Curdt, G. Waldhoff, G. Bareth, High-resolution crop surface models (CSM) and crop volume models (CVM) on field level by terrestrial laser scanning, Proceedings of SPIE - the International Society for Optical Engineering, Beijing, 2009.
[148] C.L. McCarthy, N.H. Hancock, S.R. Raine, Applied machine vision of plants: a review with implications for field deployment in automated farming operations, Intel. Serv. Robot. 3 (2010) 209–217.
[149] J.U.H. Eitel, T.S. Magney, L.A. Vierling, T.T. Brown, D.R. Huggins, LiDAR based biomass and crop nitrogen estimates for rapid, non-destructive assessment of wheat nitrogen status, Field Crop. Res. 159 (2014) 21–32.
[150] J.U.H. Eitel, T.S. Magney, L.A. Vierling, G. Dittmar, Assessment of crop foliar nitrogen using a novel dual-wavelength laser system and implications for conducting laser-based plant physiology, ISPRS J. Photogrammetry Remote Sens. 97 (2014) 229–240.
[151] J.U.H. Eitel, T.S. Magney, L.A. Vierling, H.E. Greaves, G. Zheng, An automated method to quantify crop height and calibrate satellite-derived biomass using hypertemporal lidar, Remote Sens. Environ. 187 (2016) 414–422.
[152] H.E. Greaves, L.A. Vierling, J.U.H. Eitel, N.T. Boelman, T.S. Magney, C.M. Prager, K.L. Griffin, Estimating aboveground biomass and leaf area of low-stature Arctic shrubs with terrestrial LiDAR, Remote Sens. Environ. 164 (2015) 26–35.
[153] D. Hoffmeister, G. Waldhoff, C. Curdt, N. Tilly, J. Bendig, G. Bareth, Spatial variability detection of crop height in a single field by terrestrial laser scanning, in: J.V. Stafford (Ed.), Precision Agriculture'13, Wageningen Academic Publishers, Wageningen, 2013.
[154] D. Hoffmeister, G. Waldhoff, W. Korres, C. Curdt, G. Bareth, Crop height variability detection in a single field by multi-temporal terrestrial laser scanning, Precis. Agric. 17 (2016) 296–312.
[155] J.J. Pittman, D.B. Arnall, S.M. Interrante, C.A. Moffet, T.J. Butler, Estimation of biomass and canopy height in bermudagrass, alfalfa, and wheat using ultrasonic, laser, and spectral sensors, Sensors 15 (2015) 2920–2943.
[156] G. Zheng, L.M. Moskal, Computational-geometry-based retrieval of effective leaf area index using terrestrial laser scanning, IEEE Trans. Geosci. Remote Sens. 50 (2012) 3958–3969.
[157] L. Cao, N.C. Coops, Y. Sun, H. Ruan, G. Wang, J. Dai, G. She, Estimating canopy structure and biomass in bamboo forests using airborne LiDAR data, ISPRS J. Photogrammetry Remote Sens. 148 (2019) 114–129.
[158] I. Colomina, P. Molina, Unmanned aerial systems for photogrammetry and remote sensing: a review, ISPRS J. Photogrammetry Remote Sens. 92 (2014) 79–97.
[159] T. Sakamoto, A.A. Gitelson, A.L. Nguy-Robertson, T.J. Arkebauer, B.D. Wardlow, A.E. Suyker, S.B. Verma, M. Shibayama, An alternative method using digital cameras for continuous monitoring of crop status, Agric. For. Meteorol. 154–155 (2012) 113–126.
[160] N. Tilly, D. Hoffmeister, Q. Cao, S.Y. Huang, L.-W. V, Y.X.,B.G. Miao, Multitemporal crop surface models: accurate plant height measurement and biomass estimation with terrestrial laser scanning in paddy rice, J. Appl. Remote Sens. 8 (2014) 083671–083692.
[161] K.E. Anderson, N.F. Glenn, L.P. Spaete, D.J. Shinneman, D.S. Pilliod, R.S. Arkle, S.K. McIlroy, D.R. Derryberry, Estimating vegetation biomass and cover across large plots in shrub and grass dominated drylands using terrestrial lidar and machine learning, Ecol. Indicat. 84 (2018) 793–802.
[162] J. Bendig, A. Bolten, S. Bennertz, J. Broscheit, S. Eichfuss, G. Bareth, Estimating biomass of barley using crop surface models (CSMs) derived from UAV-based RGB imaging, Rem. Sens. 6 (2014) 10395–10412.
[163] S. Crommelinck, B. Höfle, Simulating an autonomously operating low-cost static terrestrial LiDAR for multitemporal maize crop height measurements, Rem. Sens. 8 (2016) 205.
[164] J. Geipel, J. Link, W. Claupein, Combined spectral and spatial modeling of corn yield based on aerial images and crop surface models acquired with an unmanned aircraft system, Rem. Sens. 6 (2014) 10335–10355.
[165] J. Bendig, K. Yu, H. Aasen, A. Bolten, S. Bennertz, J. Broscheit, M.L. Gnyp, G. Bareth, Combining UAV-based plant height from crop surface models, visible, and near infrared vegetation indices for biomass monitoring in barley, Int. J. Appl. Earth Obs. Geoinf. 39 (2015) 79–87.
[166] F. Holman, A. Riche, A. Michalski, M. Castle, M. Wooster, M. Hawkesford, High throughput field phenotyping of wheat plant height and growth rate in field plot trials using UAV based remote sensing, Rem. Sens. 8 (2016) 1031.
[167] G. Bareth, J. Bendig, N. Tilly, D. Hoffmeister, H. Aasen, A. Bolten, A comparison of UAV- and TLS-derived plant height for crop monitoring: using polygon grids for the analysis of crop surface models (CSMs), Photogramm. Fernerkund. Geoinf. 2 (2016) 85–94.
[168] B. Höfle, Radiometric correction of terrestrial LiDAR point cloud data for individual maize plant detection, IEEE Geosci. Remote Sens. Lett. 11 (2014) 94–98.
[169] M. Hämmerle, B. Höfle, Direct derivation of maize plant and crop height from low-cost time-of-flight camera measurements, Plant Methods 12 (2016) 50–62.
[170] K.C. Swain, S.J. Thomson, H.P.W. Jayasuriya, Adoption of an unmanned helicopter for low-altitude remote sensing to estimate yield and total biomass of a rice crop, Trans. ASABE (Am. Soc. Agric. Biol. Eng.) 53 (2010) 21–27.
[171] M. Wu, C. Yang, X. Song, W. Hoffmann, W. Huang, Z. Niu, C. Wang, W. Li, Evaluation of orthomosics and digital surface models derived from aerial imagery for crop type mapping, Rem. Sens. 9 (2017) 239.
[172] E. Honkavaara, H. Saari, J. Kaivosoja, I. Pölönen, T. Hakala, P. Litkey, J. Mäkynen, L. Pesonen, Processing and assessment of spectrometric, stereoscopic imagery collected using a lightweight UAV spectral camera for precision agriculture, Rem. Sens. 5 (2013) 5006–5039.
[173] S. Sankaran, L.R. Khot, C.Z. Espinoza, S. Jarolmasjed, V.R. Sathuvalli, G.J. Vandemark, P.N. Miklas, A.H. Carter, M.O. Pumphrey, N.R. Knowles, M.J. Pavek, Low-altitude, high-resolution aerial imaging systems for row and field crop phenotyping: a review, Eur. J. Agron. 70 (2015) 112–123.
[174] H. Aasen, A. Burkart, A. Bolten, G. Bareth, Generating 3D hyperspectral information with lightweight UAV snapshot cameras for vegetation monitoring: from camera calibration to quality assurance, ISPRS J. Photogrammetry Remote Sens. 108 (2015) 245–259.

[175] M. Dalponte, L. Frizzera, H.O. Ørka, T. Gobakken, E. Næsset, D. Gianelle, Predicting stem diameters and aboveground biomass of individual trees using remote sensing data, Ecol. Indicat. 85 (2018) 367–376.
[176] J. Berni, P.J. Zarco-Tejada, L. Suarez, E. Fereres, Thermal and narrowband multispectral remote sensing for vegetation monitoring from an unmanned aerial vehicle, IEEE Trans. Geosci. Remote Sens. 47 (2009) 722–738.
[177] A. Prashar, H. Jones, Infra-red thermography as a high-throughput tool for field phenotyping, Agronomy 4 (2014) 397–417.
[178] D.P. Holzworth, V. Snow, S. Janssen, I.N. Athanasiadis, M. Donatelli, G. Hoogenboom, J.W. White, P. Thorburn, Agricultural production systems modelling and software: current status and future prospects, Environ. Model. Softw 72 (2015) 276–286.
[179] A.J.W. de Wit, C.A. van Diepen, Crop model data assimilation with the Ensemble Kalman filter for improving regional crop yield forecasts, Agric. For. Meteorol. 146 (2007) 38–56.
[180] J.W. Hansen, J.W. Jones, Scaling-up crop models for climate variability applications, Agric. Syst. 65 (2000) 43–72.
[181] X. Jin, L. Kumar, Z. Li, X. Xu, G. Yang, J. Wang, Estimation of winter wheat biomass and yield by combining the AquaCrop model and field hyperspectral data, Rem. Sens. 8 (2016) 972.
[182] W.A. Dorigo, R. Zurita-Milla, A.J.W. de Wit, J. Brazile, R. Singh, M.E. Schaepman, A review on reflective remote sensing and data assimilation techniques for enhanced agroecosystem modeling, Int. J. Appl. Earth Obs. Geoinf. 9 (2007) 165–193.
[183] M. Machwitz, L. Giustarini, C. Bossung, D. Frantz, M. Schlerf, H. Lilienthal, L. Wandera, P. Matgen, L. Hoffmann, T. Udelhoven, Enhanced biomass prediction by assimilating satellite data into a crop growth model, Environ. Model. Softw 62 (2014) 437–453.
[184] T. Hank, H. Bach, W. Mauser, Using a remote sensing-supported hydro-agroecological model for field-scale simulation of heterogeneous crop growth and yield: application for wheat in central Europe, Rem. Sens. 7 (2015) 3934–3965.
[185] M. Rinaldi, G. Satalino, F. Mattia, A. Balenzano, A. Perego, M. Acutis, S. Ruggieri, Assimilation of COSMO-SkyMed-derived LAI maps into the AQUATER crop growth simulation model. Capitanata (Southern Italy) case study, Eur J Remote Sens 46 (2013) 891–908.
[186] G. Jégo, E. Pattey, S.M. Mesbah, J. Liu, I. Duchesne, Impact of the spatial resolution of climatic data and soil physical properties on regional corn yield predictions using the STICS crop model, Int. J. Appl. Earth Obs. Geoinf. 41 (2015) 11–22.
[187] Y. Zhao, S. Chen, S. Shen, Assimilating remote sensing information with crop model using Ensemble Kalman Filter for improving LAI monitoring and yield estimation, Ecol. Model. 270 (2013) 30–42.
[188] D.B. Lobell, D. Thau, C. Seifert, E. Engle, B. Little, A scalable satellite-based crop yield mapper, Remote Sens. Environ. 164 (2015) 324–333.
[189] E.M. Perry, E.M. Morse-McNabb, J.G. Nuttall, G.J. O Leary, R. Clark, Managing wheat from space: linking MODIS NDVI and crop models for predicting Australian dryland wheat biomass, IEEE J. Sel. Topics. Appl. Earth. Observ Remote. Sens. 7 (2014) 3724–3731.
[190] H. Fang, S. Liang, G. Hoogenboom, J. Teasdale, M. Cavigelli, Corn-yield estimation through assimilation of remotely sensed data into the CSM-CERES-Maize model, Int. J. Remote Sens. 29 (2008) 3011–3032.
[191] J. Huang, H. Ma, W. Su, X. Zhang, Y. Huang, J. Fan, W. Wu, Jointly assimilating MODIS LAI and ET products into the SWAP model for winter wheat yield estimation, IEEE J. Sel. Topics. Appl. Earth. Observ Remote. Sens. 8 (2015) 4060–4071.
[192] A.V.M. Ines, N.N. Das, J.W. Hansen, E.G. Njoku, Assimilation of remotely sensed soil moisture and vegetation with a crop simulation model for maize yield prediction, Remote Sens. Environ. 138 (2013) 149–164.
[193] G. Jégo, E. Pattey, J. Liu, Using Leaf Area Index, retrieved from optical imagery, in the STICS crop model for predicting yield and biomass of field crops, Field Crop. Res. 131 (2012) 63–74.
[194] Y. Ke, J. Im, J. Lee, H. Gong, Y. Ryu, Characteristics of Landsat 8 OLI-derived NDVI by comparison with multiple satellite sensors and in-situ observations, Remote Sens. Environ. 164 (2015) 298–313.
[195] R. Delécolle, S.J. Maas, M. Guérif, F. Baret, Remote sensing and crop production models: present trends, ISPRS J. Photogrammetry Remote Sens. 47 (1992) 145–161.
[196] M. Launay, M. Guerif, Assimilating remote sensing data into a crop model to improve predictive performance for spatial applications, Agric. Ecosyst. Environ. 111 (2005) 321–339.
[197] R. Ma, L. Zhang, X. Tian, J. Zhang, W. Yuan, Y. Zheng, X. Zhao, T. Kato, Assimilation of remotely-sensed leaf area index into a dynamic vegetation model for gross primary productivity estimation, Rem. Sens. 9 (2017) 188.
[198] M.E. Schaepman, Spectrodirectional remote sensing: from pixels to processes, Int. J. Appl. Earth Obs. Geoinf. 9 (2007) 204–223.
[199] X. Jin, L. Kumar, Z. Li, H. Feng, X. Xu, G. Yang, J. Wang, A review of data assimilation of remote sensing and crop models, Eur. J. Agron. 92 (2018) 141–152.
[200] C. Gilardelli, T. Stella, R. Confalonieri, L. Ranghetti, M. Campos-Taberner, F.J. García-Haro, M. Boschetti, Downscaling rice yield simulation at sub-field scale using remotely sensed LAI data, Eur. J. Agron. 103 (2019) 108–116.